How Radical are 'Radical' Photocatalysts? A Closed-Shell Meisenheimer Complex is Identified as a Super-reducing Photoreagent

Adam J. Rieth, Miguel I. Gonzalez, Bryan Kudisch, Matthew Nava, and Daniel G. Nocera*

[a] *Department of Chemistry and Chemical Biology, Harvard University, 12 Oxford Street, Cambridge, MA 02138, USA.*

ABSTRACT: Super-reducing excited states have the potential to activate strong bonds, leading to unprecedented photoreactivity. Excited states of radical anions, accessed via reduction of a precatalyst followed by light absorption, have been proposed to drive photoredox transformations under super-reducing conditions. Here we investigate the radical anion of naphthalene monoimide as a photoreductant and find that the radical doublet excited state has a lifetime of 24 ps, which is too short to facilitate photoredox activity. To account for the apparent photoreactivity of the radical anion, we identify an emissive two-electron reduced Meisenheimer complex of naphthalene monoimide, $[NMI(H)]^-$. The singlet excited state of $[NMI(H)]^-$ is a potent reductant (–3.08 V vs Fc/Fc^+), is long-lived (20 ns), and its emission can be dynamically quenched by chloroarenes to drive a radical photochemistry, establishing that it is this emissive excited state that is competent for reported C–C and C–P coupling reactivity. These results provide a mechanistic basis for photoreactivity at highly reducing potentials via singlet excited state manifolds and lays out a clear path for the development of exceptionally reducing photoreagents derived from electron-rich closed-shell anions.

INTRODUCTION

Exploring the redox potential limits accessible by photoinduced single-electron transfer can unlock new reactivity and expand the range of processes amenable to photoredox chemistry and the design of attendant synthetic methods. Using standard photocatalysts with ground state highest occupied molecular orbital (HOMO) potentials near to or more oxidizing than that of the normal hydrogen electrode (NHE = 0), bond activation energies using visible light have been practically limited to less than ~2 V in either direction.[1,2] Recently, these limits have been circumvented by shifting the ground state potential of the photocatalyst via redox processes prior to light absorption; oxidation of a precatalyst followed by light absorption generates strongly oxidizing excited states[3–6] and reduction of a precatalyst followed by light absorption can generate super-reducing excited states.[7–11] These two-photon or electrophotocatalytic processes dramatically expand the range of photo-accessible synthetic disconnections.[7–11] Additionally, because the processes are photoactivated, they are selective for single electron transfer (SET) even in cases where direct electrolysis would result in over-oxidation or -reduction.[7] Although the highly reducing nature of excited organic radical anions has long been recognized,[17,12,13] the mechanism and energetics of a process driven by a doublet excited state is quizzical as internal conversion for such a $\Delta S = 0$ nonradiative decay to a doublet ground state is exceptionally fast. Spectroscopic investigations of organic radicals have demonstrated nearly universally short excited-state lifetimes on the ps timescale,[14–19] in one case even shorter than a single vibrational period (7 fs).[20] Although electron transfer from radical anions does occur intramolecularly in covalently linked donor-acceptor systems,[21,22] the short lifetime of doublet excited states cannot support intermolecular processes of photoredox reactions as the lifetime (τ_o) of the active excited state should be longer than the average time between molecular encounters—that is $\tau_o \geq 1/k_d[sub]$ where k_d is the rate of diffusion (typically ~10^9 – 10^{10} $M^{-1}s^{-1}$), and [sub] is the concentration of substrate. For a substrate concentration of 0.1 M, an approximate lower bound for a SET process requiring diffusion is $\tau_o \geq$ 1–10 ns. Therefore, the measured excited state lifetimes of nearly all radical doublet species are orders of magnitude too short to result in productive photochemistry. Indeed, excited state spectral features with lifetimes longer than 1 ns measured for several presumptive radical anions[23,24] were later shown to instead arise from longer-lived closed shell impurities. For instance, the radical anions of both 9,10-dicyanoanthracene and anthraquinone were later found to contain the emissive byproducts cyanoanthrolate or bianthrolate, respectively.[14–19,24] Therefore, there is an imperative to better understand the nature of super-reducing radical photoreagents.[7,9,10] A proper mechanistic understanding of the origins of super-reducing photochemistry can facilitate their application in the design of photoredox methods, and expand the possibilities for bond activation via reductive SET.[25]

Here we show that for one recently reported photoelectrocatalyst, naphthlalene monoimide (NMI),[7] the photoactive component is not a radical, but a two-electron reduced species. Using a combination of cyclic voltammetry, spectroelectrochemistry, and ultrafast spectroscopy, we demonstrate that two-electron reduction of NMI produces an emissive Meisenheimer complex,[26,27] $[NMI(H)]^-[TBA]^+$ (TBA = tetrabutylammonium), which has been isolated and crystallographically characterized. Time-resolved

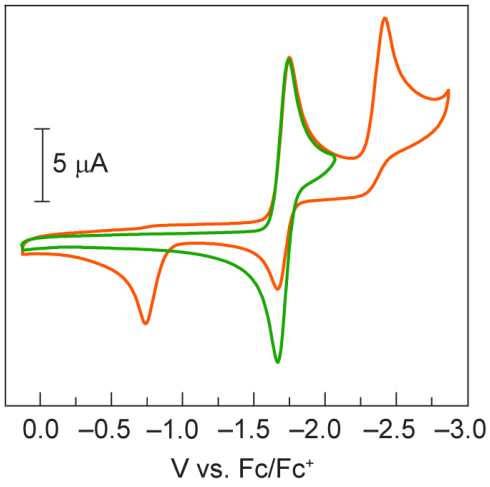

Figure 1. (**A**) Cyclic voltammograms of 1 mM NMI in 0.1 M $TBAPF_6$ propylene carbonate solution, scanning at 50 mV s^{-1} from 0.2 to –2.0 V (green) and 0.2 to –2.8 V (orange), using a glassy carbon working electrode, Pt mesh counter electrode, and leak-free Ag/AgCl reference electrode.

spectroscopy reveals that the lifetime of the doublet excited state of the radical anion ($\tau[^2NMI^{-\bullet}]^*$) is 24 ps, which is too short to participate in photoredox chemistry. By contrast, the lifetime of the singlet excited state of the Meisenheimer complex ($\tau[^1NMI(H)^-]^*$) is 20 ns. This long fluorescent lifetime together with a –3.08 V vs. Fc/Fc^+ excited state energy gives rise to super-reducing chemistry. Indeed, the emissive excited state of the doubly reduced Meisenheimer complex is dynamically quenched by haloarene substrates, and leads to the previously observed C–C and C–P coupling reactivity.[7] These results provide a clear mechanistic underpinning for super-reducing photoelectrocatalysis, laying out a path for the further development of powerfully reducing closed-shell anions as photoreagents for novel bond activation pathways.

RESULTS

Cyclic voltammetry (CV) of NMI in propylene carbonate containing 0.1 M tetrabutylammonium hexafluorophosphate ($TBAPF_6$) revealed two reductive events (Figure 1). The first reduction wave occurs at –1.7 V vs Fc/Fc^+ and is fully reversible, so long as the sweep potential is limited to avoid the second reductive wave (Figure 1, green). The first reductive event corresponds to a single electron transfer to reversibly form the NMI radical anion, as previously observed.[7,18] The second reductive feature is irreversible, at approximately –2.6 V (Figure 1, orange), and also corresponds to a one-electron process, coupled to a chemical step. The appearance of this irreversible reductive wave is accompanied by the emergence of an oxidative feature at –0.7 V, as well as a decrease in the peak height for reoxidation of the previously reversible feature at –1.7 V. Increasing the scan rate results in the formation of two distinct oxidation features near –0.7 V, as well as partial reversibility of the –0.7 V feature upon reduction (Figure S1, S2). The cyclic voltammetry features are not altered after 10 cycles (Figure S3). After scanning past –2.6 V, the reversibility of the radical anion feature at –1.7 V can be recovered when the scan is limited to –2.0 V on the subsequent cycle (Figure S4).

Figure 2 shows spectroelectrochemistry data when the working electrode in a two-compartment H-cell is polarized to –2.3 V vs. Fc/Fc^+, which is sufficiently beyond the first wave to drive the one

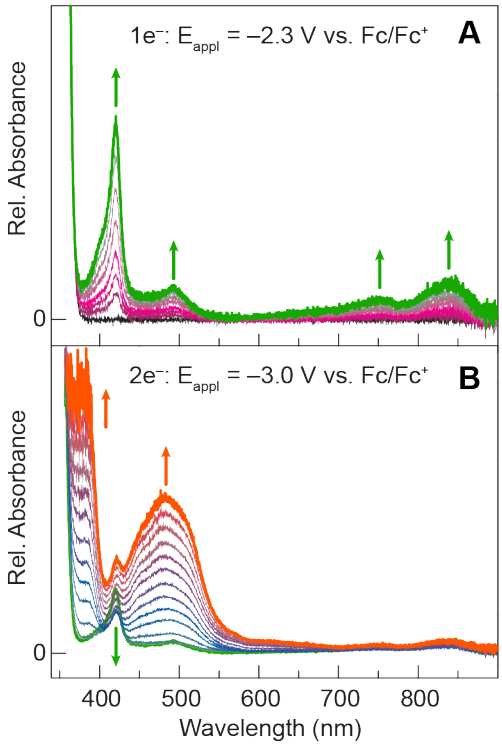

Figure 2. UV-visible spectroelectrochemistry of 1 mM NMI in 0.1 M $TBAPF_6$ dimethylacetamide solution. The Pt working electrode was poised at the $1e^-$ reducing potential of E_{appl} = –2.3 V (**A**) and the $2e^-$ reducing potential of E_{appl} = –3.0 V (**B**).

electron reduction of NMI. Prominent absorption features appear at 422 and 493 nm, as well as weaker absorption signals at 750 and 850 nm (Figure 2A, green), all of which are characteristic of a naphthalene imide radical anion.[18] Bulk electrolysis at –2.3 V vs. Fc/Fc^+ in a W-cell generated a bright lime green solution in the catholyte (Figure S5), with the same absorption features in Figure 2A. Examination of this electrolyzed solution by ultrafast transient absorption (λ_{exc} = 420 nm) revealed a bleach signal as well as an excited state absorption feature, both of which decay with a lifetime of 24 ps (Figures 3A, 3B). This result is in agreement with previous measurements of rylene imide radical anion excited states.[18]

Figure 2B shows the spectroelectrochemistry of NMI when the applied potential in Figure 2A is shifted more reducing, to –3.0 V, beyond the second reductive wave in CV. Strong absorption features at 385 nm and 490 nm grow in (Figure 2B, orange) with the concomitant disappearance of the NMI radical anion absorption features. Bulk electrolysis in a W-cell at –3.0 V vs. Fc/Fc^+ generated a bright orange solution in the catholyte, with visible green emission at λ_{max} = 550–600 nm (Figure 3C and Figure S5), just beyond the lowest energy absorption feature of the two-electron reduced NMI. A fluorescence excitation spectrum (Figure 3C, light orange dash) coincides with the absorption features of the doubly reduced NMI species, with the most intense emission arising from excitation of the absorption bands at 385 nm and 490 nm. A lower-intensity emission with λ_{max} = 550–600 nm is also observed for samples electrolyzed at –2.3 V, and its excitation spectrum also matches that of the two-electron reduced NMI (Figure S7). This result is consistent with the CV in Figure 1, which shows the onset of the second reduction occurs at –2.3 V. In view of the lowest energy absorption of the NMI radical anion, emission, if present, would be expected to occur beyond 850 nm. However, no emission is observed arising from the

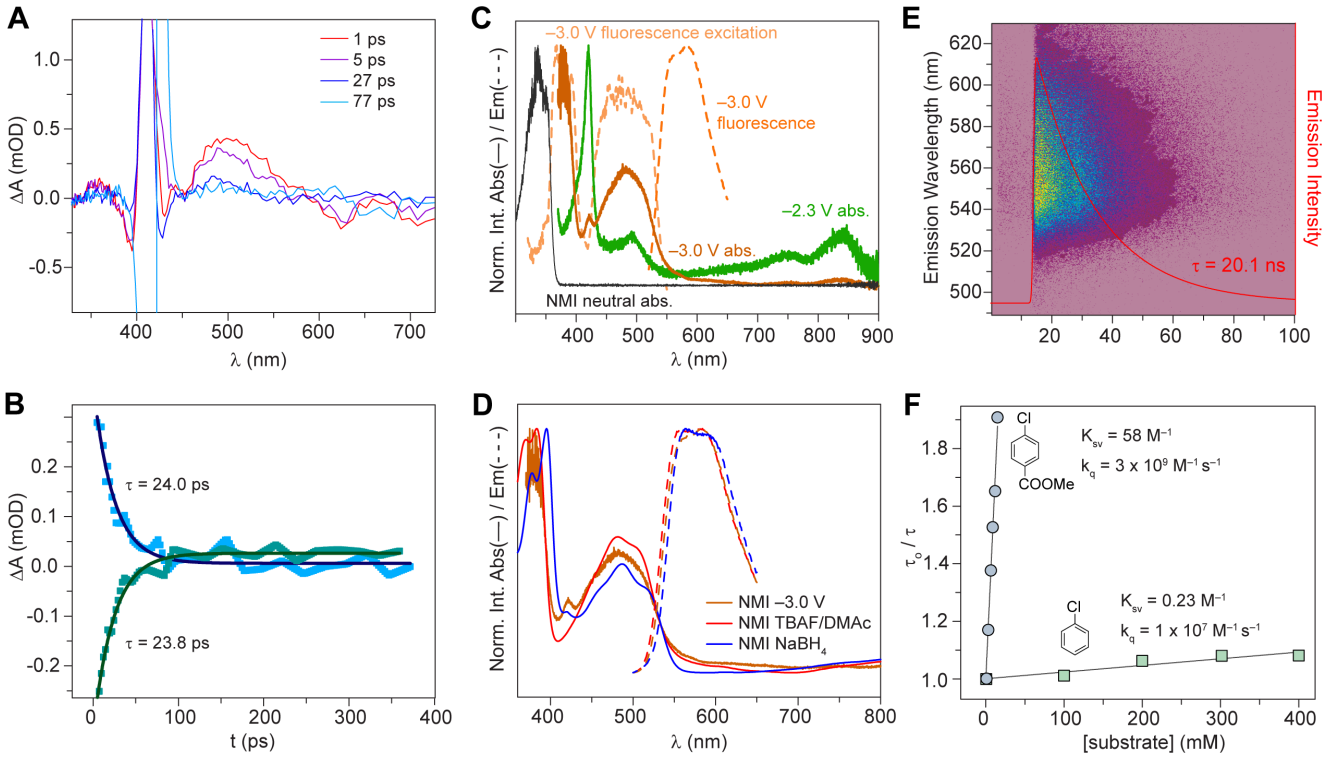

Figure 3. (**A**) Transient absorption spectra for NMI electrolyzed at –2.3 V results in a transient absorption feature at λ_{max} = 500 nm and a bleaching signal between 380 to 425 nm; the bleach signal is interrupted by a sharp feature at 420 nm due to the excitation pump used to excite the most prominent absorptive feature of the NMI radical anion. (**B**) Single exponential decay fits (red lines) to the transient absorption data in panel **A** for the excited state absorption intensity averaged between 495–525 nm (■, light blue) and the bleach feature between 385–395 nm (■, sea green), both of which exhibit 24 ps lifetimes. (**C**) Normalized absorption spectra of NMI (black), NMI electrolyzed at –2.3 V (one-electron reduced species, green), NMI electrolyzed at –3 V (two-electron reduced species, burnt orange), overlayed with the normalized emission spectrum of the –3.0 V electrolyzed sample (orange dash) and the excitation scan for the emission at 600 nm (light orange dash). (**D**) Normalized absorption (solid) and emission (dashed) spectra for NMI electrolyzed at –3.0 V vs. Fc/Fc^+ (burnt orange), NMI treated with TBAF in DMAc (pink), and NMI treated with $NaBH_4$ in DME (blue). (**E**) fs-pumped streak camera emission image (λ_{exc} = 480 nm) for NMI treated with TBAF in DMAc. Colors represent photon counts (purple is low and red is high). The red line shows a mono-exponential fit of data averaged in a 540–560 nm spectral window. (**F**) Dynamic Stern-Volmer quenching plots of solutions of NMI treated with TBAF in DMAc in the presence of 4-methylchlorobenzoate or chlorobenzene (fitted data presented in Figures S9 and S10).

NMI radical anion, even when excited at its peak absorption wavelength λ_{max} = 420 nm and the emission detection wavelength is scanned into the infrared spectral region (λ_{det} = 800–1500 nm, InGaAs detector) (Figure S8).

NMI may be reduced chemically using either fluoride-mediated solvent oxidation with tetrabutylammonium fluoride (TBAF) in N,N′-dimethylacetamide (DMAc) or treatment with $NaBH_4$ in dimethoxyethane (DME). For both reduction reactions, the absorption and emission spectra of the reduced product match those obtained for the electrochemically two-electron reduced NMI (Figure 3D). Emission lifetime measurements were performed on NMI solutions in DMAc treated with TBAF using a fs-pumped streak camera (Figure 3E). The data were averaged in the 540 to 560 nm window and fitted to a single exponential decay to furnish a lifetime of 20.1 ns (Figure 3E, red line).

Addition of chloroarene substrates to NMI treated with TBAF in DMAc resulted in dynamic quenching of the emission lifetime (Figures S9 and S10). Figure 3F shows well-behaved Stern-Volmer kinetics as measured by lifetime quenching. For methyl-4-chlorobenzoate the quenching rate constant is k_q =3 × 10^9 M^{-1} s^{-1}, and for the more challenging reduction of chlorobenzene, the quenching rate constant is reduced to k_q = 10^7 M^{-1} s^{-1}.

Isolation of the doubly reduced, emissive NMI species proved possible via treatment of NMI with $NaBH_4$ in dimethoxyethane. Anion exchange of the resulting product with tetrabutylammonium chloride resulted in a bright orange solid. ^{1}H and Heteronuclear Single Quantum Correlation – Distortionless Enhancement by Polarization Transfer (HSQC-DEPT) NMR experiments offered initial evidence of a hydride-reduced naphthalene ring: the phase of the resonance near 4.1 ppm in ^{1}H NMR indicates a CH_2 group, and not a CH or CH_3 group (Figure S11). Experimental NMR spectra were consistent with *ab initio* structure and NMR chemical shift calculations of two NMI hydride addition isomers, *ortho*- and *para*-$[NMI(H)]^-$ (Figures S12–S13, Tables S9–S10 for ^{1}H, S14–S15 for ^{13}C, and S18–S19, Figure S23 for NMR peak assignments). Additional calculations revealed that the NMR data is inconsistent with two other conceivable isomers, *meta*- and *carbo*-$[NMI(H)]^-$ (Tables S11–S12 for ^{1}H, S16–S17 for ^{13}C). Treatment of NMI with $NaBD_4$, followed by oxidation in air, leads to a partially deuterated naphthalene ring, evidenced by reduced integrated intensity in ^{1}H NMR largely at the *ortho*-, though also at the *para*-position (Figure S14).

Recrystallization of the $NaBH_4$-reduced NMI via slow diffusion of diethyl ether into a toluene solution of the product resulted in orange blade-like crystals suitable for single-crystal X-ray diffraction

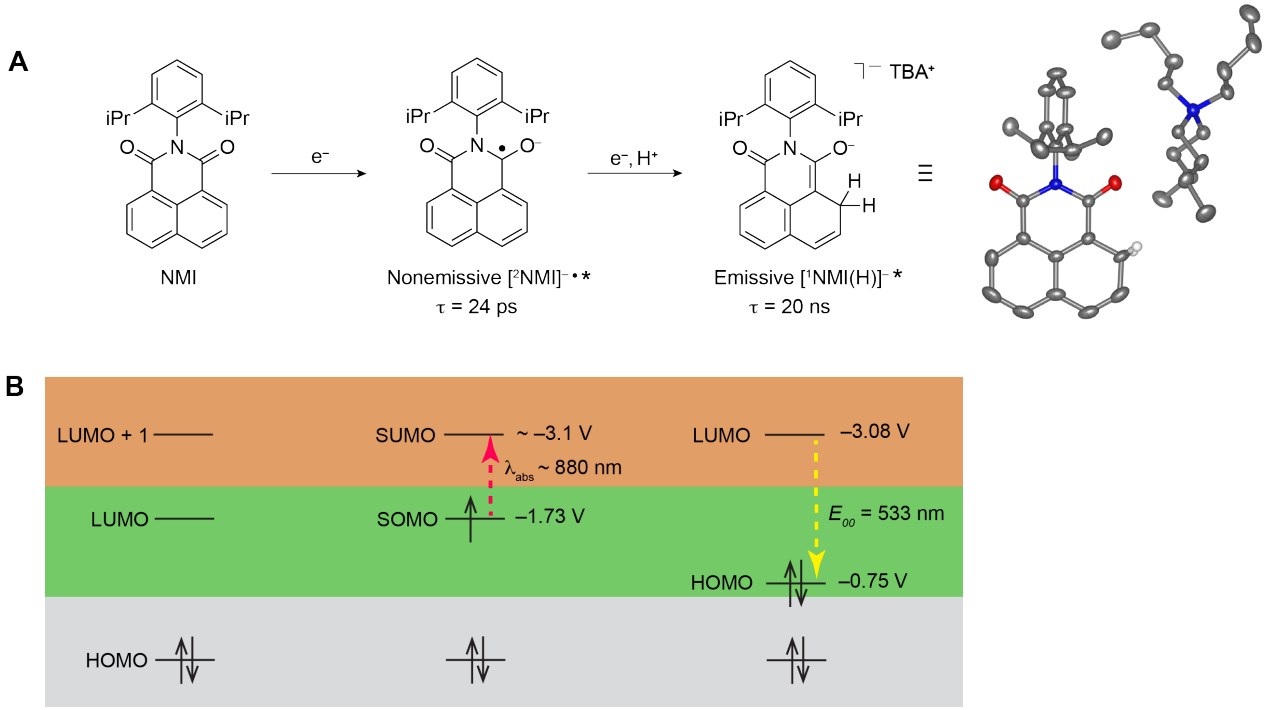

Figure 4. (**A**) Single-electron reduction of naphthalene monoimide (NMI) furnishes the radical anion with a doublet excited state ($[^2NMI^{-\bullet}]^*$) lifetime of 24 ps. A second electron transfer followed by protonation furnishes a two-electron reduced, emissive Meisenheimer complex with a singlet excited state ($[^1NMI(H)^-]^*$) lifetime of 20 ns. Right: crystal structure of $[NMI(H)]^-[TBA]^+$: C, gray; N, blue; O, red; H, white. H atoms except those on the sp^3 carbon of the naphthalene ring are omitted and disorder is removed for clarity. Thermal ellipsoids shown at 50% probability. (**B**) Simplified energy level diagram of the NMI system; all potentials given vs. Fc/Fc^+. Energy levels for each species is aligned with the compounds in **A**. SOMO = singly occupied molecular orbital. SUMO = singly unoccupied molecular orbital. Energetics of $[NMI(H)]^-$ are assigned in Figure S24.

analysis (Figure S15). Figure 4A shows the structure of the product, which corresponds to a reduced anionic NMI species with a charge-balancing $[TBA]^+$ countercation. A slight twist was evident in the imide ring, with a dihedral angle of 2.5°. Further examination of the structure revealed that the two carbon atoms at the 2- and 7-positions of the reduced naphthalene ring exhibited C–C bond lengths that were longer than expected for sp^2-hybridized carbon atoms. In addition, the residual electron density around these carbon atoms suggested the presence of both $C(sp^3)H_2$ and $C(sp^2)H$ hydrogen atoms. Accordingly, the structure was best refined with one sp^3 hybridized carbon and one sp^2 hybridized carbon disordered over the 2- and 7-positions. Consistent with the quinodal structure of a hydride-reduced Meisenheimer complex, the average carbonyl C–O bond distances were lengthened by 0.035(6) Å and the average C–C bond distances between the carbonyl groups and the reduced naphthalene ring were shortened by 0.048(5) Å with respect to the independently crystallized neutral NMI (Table S1). These relative changes in bond lengths are consistent with *ab initio* calculations for NMI and *ortho*-$[NMI(H)]^-$ (Figures S16 and S17, and Tables S3 and S4). Other structures of formal hydride addition products of NMI were also optimized, including *para*-, *meta*-, and *carbo*-$[NMI(H)]^-$, which did not match the crystallographic bond length changes (Figures S18-S20 and Tables S5-S7)

A cyclic voltammogram of the isolated $[NMI(H)]^-[TBA]^+$ reveals a prominent irreversible oxidative wave near –0.7 V (Figure S6), matching the features observed upon the two-electron reduction of the neutral NMI. Additionally, using $[NMI(H)]^-[TBA]^+$ as a stoichiometric photoreagent, the reactivity previously reported to be due to the NMI radical anion is reproduced.[7] Specifically, treatment of $[NMI(H)]^-[TBA]^+$ with stoichiometric methyl-4-chlorobenzoate in C_6D_6 resulted in no reaction in the dark (Figure S25). Upon 440 nm irradiation, the reductive homocoupling product dimethyl-biphenyl-4,4'-dicarboxylate is observed as the major product, along with a smaller amount of the hydrodehalogenation product methyl benzoate (Figure S25). In the presence of excess N-methyl pyrrole, the C–C coupling product resulting from benzoate radical addition to N-methyl pyrrole is also observed (Figure S26). In the presence of 5 equiv. triethylphosphite, the C–P coupling product methyl 4-(diethoxyphosphoryl)benzoate was obtained as the major product (Figures S27, S28).

DISCUSSION

Figure 4A summarizes the results of NMI redox chemistry and attendant excited state energetics and dynamics. NMI is reduced at –1.73 V vs. Fc/Fc^+ and when the voltammetry scan range is limited to less than –2.3 V, the one-electron wave is reversible, indicating the formation of a stable radical anion, $NMI^{-\bullet}$ (Figure 1, green). Bulk electrolysis of NMI at –2.3 V vs. Fc/Fc^+ yields the well-defined and characteristic absorption spectrum of $NMI^{-\bullet}$ shown in Figure 2A (green trace). The absorption spectrum of solutions in the dark are indefinitely stable in the glovebox, allowing for the $NMI^{-\bullet}$ excited state properties to be examined upon its production by bulk electrolysis. The absence of emission from solutions of the radical anion is noteworthy, as the quantum yield for emission is:

$$\Phi_e = k_r/(k_r + k_{nr}) \quad (1)$$

where k_r is the rate of radiative relaxation and k_{nr} is the rate of nonradiative relaxation. The lack of emission is indicative of fast non-radiative decay subject to the condition that $k_{nr} >> k_r$. This contention is verified by transient absorption spectroscopy (Figure

3A), which is able to capture the dynamics of the radical anion inasmuch as there is no emission signal available to monitor excited state decay kinetics. The bleaching signal as a result of ground state depletion (λ = 385–395 nm) recovers with the same lifetime (24 ps) as the decay of the excited state absorption signal (λ = 495–525 nm) of the NMI radical anion. A 24 ps lifetime of the radical anion excited state (Figure 3B) is too short to support bimolecular chemistry. Assuming an electron transfer rate constant at the diffusion limit of 10^{10} M^{-1} s^{-1}, at the concentrations that substrate has been employed for photoreactivity (0.1 M), the chromophore will encounter a substrate molecule on average every 1 ns. Therefore, with a lifetime of 24 ps, ~42 lifetimes of the excited state will pass between chromophore-substrate interactions, resulting in an excited state concentration of ~10^{-19} times the original concentration of excited state. The passage of so many excited state lifetimes between chromophore-substrate collisions would give rise to a vanishingly small quantum yield that is too low to support observed photoredox conversion yields, which are achieved in a timescale of hours. In the absence of a viable photoredox chemistry of the radical anion, we sought to identify the species responsible for effecting the single-electron reductive chemistry of haloarenes, as such a photoreagent must possess potent reducing properties, which could be useful for a wide range of chemical conversions.

Extending the cathodic window of CV scans to more negative potential, a second wave is observed beyond the NMI radical anion (Figure 1, orange). The wave in Figure 1 is extremely informative. The cathodic current matches that observed for reduction of NMI to $NMI^{-\bullet}$, thus indicating a one-electron process. Moreover, the irreversibility of the second reductive wave is a characteristic of an EC process[28] in which NMI radical anion undergoes a facile chemical reaction following the addition of an electron. The observation of a remnant amount of radical anion upon the anodic scan likely results from a limiting proton inventory needed for the chemical step of the EC process (vide infra). The anodic wave at $E_{p,a}$ = –0.65 V (orange trace) is associated with the product of the EC process of the NMI radical anion. At fast scan rates, the wave exhibits quasi-reversible behavior (Figure S2), indicative of a redox process associated with the product of the two-electron EC process of NMI. These data indicate that deprotonation of the neutral NMI(H) species is rapid and occurs within the electrode double layer. Deprotonation results in the NMI radical anion, which, at –0.65 V, is also rapidly oxidized to form NMI.

Spectroelectrochemistry of NMI solutions under an applied voltage of –3.0 V reveals the two-electron species may cleanly be generated and is stable in the absence of oxygen, as indicated by the permanence of the absorption spectrum (Figure 2B). Bulk electrolysis of the NMI solutions at –3.0 V generates an orange solution with a pronounced emission band, $\lambda_{em,max}$ = 563 nm (Figure 3C). Excitation scans reveal that the fluorescence tracks the 385 and 490 nm absorption envelopes of the two-electron reduced NMI species (Figure 3C). We note that the excitation spectrum in Figure 3C is the same as that recently assigned to an excitation spectrum of a purported quartet excited state of $NMI^{-\bullet}$.[29] As the excitation spectrum is not that of the NMI radical anion, our result establishes that emission originates from the excited state of the two-electron reduced NMI species and not from either a spin-allowed or a spin forbidden excited state of the radical anion.

The cyclic voltammetry and spectroelectrochemistry results suggested that the doubly reduced NMI species generated from the EC process could be chemically generated and isolated. Treatment of NMI with $NaBH_4$, followed by cation exchange, allowed for the isolation and crystallographic characterization of $[NMI(H)]^-$ $[TBA]^+$ (Figures 4 and S15). NMR characterization and comparison to DFT NMR shift calculations indicated the likely presence of two isomers, wherein the sp^3 carbon on the naphthalene ring is either *ortho-* or *para-* to the imide ring (Figures S11 and S23, Tables S18 and S19). Crystallographic refinement gave bond metrics consistent with the *ortho-* isomer (Table S1, Figure S15). Cyclic voltammetry of the isolated $[NMI(H)]^-[TBA]^+$ revealed the same peaks as for neutral NMI, with a prominent initial oxidative wave at –0.7 V vs. Fc/Fc^+ (Figure S6). These results confirm the assignment of the two-electron reduced NMI observed in electrochemistry as the hydride-reduced species, $[NMI(H)]^-$.

NMI may also be conveniently reduced by DMAc. Treatment of rylene imides with fluoride sources in some polar aprotic solvents was previously reported to result in one electron reduction, in the dark.[34,35] The mechanism of this process has been debated in the literature, with initial reports suggesting direct fluoride oxidation[34,30] later revised by reports of fluoride-mediated solvent oxidation,[35] wherein a proton-coupled electron transfer (PCET) process involving solvent deprotonation and formation of bifluoride is concomitant with electron transfer from solvent to rylene imide. In the case of rylene bisimides, for which two-electron reductions are fully reversible, this process was demonstrated to terminate at one electron.[35,31] Here, for naphthalene monoimide, fluoride treatment in DMAc results in the formation of the two-electron reduced NMI, with absorption and emission spectra matching those of the doubly reduced species by spectroelectrochemistry. The same spectra are obtained for treatment of NMI with hydride transfer reagents such as $NaBH_4$ (Figure 3D). We envision three plausible mechanisms for the generation of $[NMI(H)]^-$ by fluoride treatment of DMAc: solvent deprotonation followed by direct hydride transfer from solvent to NMI, solvent anion σ-addition to NMI followed by hydride elimination, or fluoride-mediated solvent oxidation to generate the NMI radical anion, followed by disproportionation. Other mechanisms involving nucleophilic fluoride addition to NMI, similar to that proposed in a recent publication,[10] may also be operative.

Generation of $[NMI(H)]^-$ by TBAF in DMAc proved to be a convenient method to study the emissive lifetime and dynamic quenching with substrates. The lifetime of the emissive excited state of $[NMI(H)]^-$, 20 ns, is just long enough to react in a useful fashion in solution limited by diffusion. With this lifetime, reactivity requires high substrate concentrations for efficient quenching. The high excited state reduction potential of $[NMI(H)]^-$ allows it to react with haloarenes. The two-electron reduced excited state species is dynamically quenched by aryl chlorides previously used as substrates for electrophotocatalytic C–C and C–P coupling reactions. We show that the fluorescence at 550 nm is quenched dynamically, indicating that substrate and excited state photocatalyst directly interact, providing an additional relaxation pathway for the photocatalyst which reduces its lifetime. The quenching rate for 4-methylchlorobenzoate, on the order of 10^9 M^{-1} s^{-1}, is near the diffusion limit (Figures 3F and S8). However, the substantially slower rate for chlorobenzene, on the order of 10^7 M^{-1} s^{-1} (Figures 3F and S9), indicates that this substrate is approaching the limit of redox potential for the excited state.

The reducing power of the $[NMI(H)]^-$ excited state, $[NMI(H)]^{-*}$, may be determined from a Latimer diagram (Figure 24C). With properly assigned spectral properties, the overlap of the

absorption and emission profiles of the two-electron reduced species (Figure S24B) furnishes an E_{00} value of 533 nm, establishing an excited state energy of 2.33 eV. The reduction potential of the two-electron reduced NMI is approximated by the anodic wave at –0.75 V vs. Fc/Fc^+ in cyclic voltammetry (Figure S24A), furnishing a reduction potential of $E([NMI(H)]^{0/-}$ = –3.08 V vs Fc^+/Fc (Figure S24C). The energetics of the $[NMI(H)]^-$ anion are summarized on the energy level diagram of Figure 4B together with those of its NMI and NMI radical anion congeners.

As indicated by the Stern-Volmer quenching results and excited state redox potential, $[NMI(H)]^{-*}$ is super-reducing, capable of supporting SET to haloarene substrates. Treatment of $[NMI(H)]^-$ $[TBA]^+$ with stoichiometric methyl-4-chlorobenzoate in C_6D_6, along with 440 nm light and the radical traps N-methyl pyrrole or triethylphosphite resulted in C–C and C–P coupled products (Figures S26–S28) that recapitulated the photon-mediated reactivity previously attributed to the NMI radical anion. Additionally, in the absence of a radical trap, irradiated solutions of methyl-4-chlorobenzoate and $[NMI(H)]^-[TBA]^+$ produced the aryl homocoupling product dimethyl-biphenyl-4,4′-dicarboxylate, along with a smaller amount of the hydrodehalogenation product methyl benzoate (Figure S25). The biphenyl product is the plausible result of radical–radical coupling, which, in the absence of a transition metal catalyst, normally requires high radical concentrations.

The use of electrophotochemistry to generate NMI radical anion is not selective, as $[NMI(H)]^-$ may also be produced. The onset potential of the EC process is at –2.3 V vs Fc/Fc^+. Consequently, the use of –2.3 V in electrophotochemistry methods will result in a Nernstian production of $[NMI(H)]^-$. The issue of non-selective production of the NMI radical anion is exacerbated by employing constant-current electrolysis, as has routinely been utilized to date, to generate the photoactive NMI species because the applied potential at the working electrode is uncontrolled. In a constant-current electrolysis, the working electrode is driven to a potential needed to maintain a constant current and thus will greatly exceed the onset potential of the EC process of the radical anion. Indeed, when the applied potential to the working electrode was controlled (not constant-current but constant potential) and set to a value slightly beyond the first reductive wave of NMI, product yields were substantially attenuated.[7] In line with these results, we observe a small amount of fluorescence from a sample electrolyzed at –2.3 V. The fluorescence excitation scan is not that of the NMI radical anion but matches that of the UV-vis spectrum of $[NMI(H)]^-$ (Figure S7). Thus, under constant current electrophotochemistry conditions, $[NMI(H)]^-$ is invariably formed and it is this species that is responsible for the observed photoreactivity.

Highly colored Meisenheimer complexes have a rich chemistry.[26,27] They are key intermediates in S_NAr chemistry,[32] formed as σ-addition complexes of nucleophiles with arenes, and hydride Meisenheimer complexes have been implicated in biological metabolic pathways.[33] We demonstrate herein the utility of Meisenheimer complexes as super-reducing photocatalysts. Beyond the hydride σ-complex of NMI reported here, other nucleophiles could produce similar Meisenheimer adducts. Fluoride-mediated solvent oxidation may result in dimethylacetamidyl (from DMAc) or dimsyl (from DMSO) anion addition to NMI.[34,35] Additionally, of possible relevance to several photochemical cycles invoking two-photon radical anion photocatalysis, a photon-mediated formation of a triethylamine (TEA) σ-complex may be envisioned wherein photooxidation of TEA followed by deprotonation produces a radical pair consisting of the NMI radical anion and the neutral TEA radical. A σ-complex formed from this radical pair is another possible photoactive Meisenheimer adduct. Moreover, the reduction potential for $[NMI(H)]^-$ is 1 V positive of the reduction potential for the formation of the NMI radical anion, allowing for the possibility of $[NMI(H)]^-$ to function as a useful two-electron hydride transfer reagent. Accordingly, the development of Meisenheimer complexes may produce a palate of useful powerfully reducing one- and two-electron photoreagents.

The results reported herein for the NMI Meisenheimer complex may likely be generalized to organic transformations reported to be driven by radical anion excited states, as a preponderance of results demonstrate such doublet excited states to be too short-lived[14–19] to participate in bimolecular reactions with substrates. For instance, hydrodehalogenation at potentials more reducing than –2.0 V vs. saturated calomel electrode (SCE), initially proposed to be driven by the perylene diimide (PDI) radical anion excited state,[36] is likely due to a closed-shell photoactive species that is formed by oxidative coupling between PDI and various substrates.[37,38] Chloroarene electrophotoreductions have also been reported to result from a photoactive species that is proposed to be the radical anion of dicyanoanthracene.[9] However, the non-emissive dicyanoanthracene radical anion is frequently accompanied by emissive anthrolate or cyanoanthrolate impurities resulting from a bimolecular oxidation reaction of the neutral species.[12,17,39] Such closed-shell anthrolate anions are known to be competent photocatalysts for very similar photoreductions of chloroarenes.[40–42] In summary, the ultrafast relaxation resulting from internal conversion of doublet excited states to a doublet ground states suggests that synthetically useful photochemically active radical species would be extraordinary, as opposed to their reaction to produce closed shell species in which photoredox processes are driven from the more common singlet/triplet lowest energy excited state manifold.

CONCLUSIONS

Spectro/electrochemical data combined with ultrafast transient absorption and emission spectroscopies demonstrates that the photoactive NMI species is a two-electron reduced singlet excited state $[NMI(H)]^{-*}$, and not the excited state of the radical anion $NMI^{-\bullet}$. The closed-shell electron rich photocatalyst results from two sequential one electron reductions of NMI, followed by a chemical step, which furnish a hydride. Whereas the short lifetime of 24 ps (Figures 3A, 3B) of the radical anion doublet excited state precludes intermolecular electron transfer, as imposed by diffusional limitations, the two-electron closed shell singlet excited state $[NMI(H)]^{-*}$ possesses a lifetime of 20 ns, which is typical of closed shell singlet excited states. This sufficiently long-lived excited state together with an exceptional excited state reduction potential bestows $[NMI(H)]^-$ with the properties to react with aryl halide substrates and effect C–C and C–P bond coupling, initiated by single electron transfer.

There are few excited state species with such super-reducing properties and sufficiently long lifetime to drive photoredox events. To this end, $[NMI(H)]^-$ should find utility as a reagent for a variety of photochemical transformations that require the activation of strong bonds. Finally, the work described herein highlights that doublet excited states are generally too short-lived to support

photoredox chemistry driven by electronically excited radical anions. We suspect that for systems in which radical anions have been proposed to drive photoredox chemistry, it may be prudent to reconsider the possibility of a more stable, closed shell, super-reducing species. Such re-evaluation will be useful for future elaboration of the role of super-reducing excited state species underpinning new synthetic methodologies.

ASSOCIATED CONTENT

Supporting Information

Experimental procedures, synthetic methods, characterization, crystallographic data, .cif structure files, Figures S1–S28, and Tables S1–S19. The Supporting Information is available free of charge on the ACS Publications website.

AUTHOR INFORMATION

Corresponding Author

Daniel G. Nocera – Department of Chemistry and Chemical Biology, Harvard University, 12 Oxford Street, Cambridge, MA 02138–2902; orcid.org/0000-0001-5055-320X; E-mail: dnocera@fas.harvard.edu.

Authors

Adam J. Rieth – Department of Chemistry and Chemical Biology, Harvard University, 12 Oxford Street, Cambridge, MA 02138–2902; orcid.org/0000-0002-9890-1346.

Miguel I. Gonzalez – Department of Chemistry and Chemical Biology, Harvard University, 12 Oxford Street, Cambridge, MA 02138–2902; orcid.org/0000-0003-4250-9035

Bryan Kudisch – Department of Chemistry and Chemical Biology, Harvard University, 12 Oxford Street, Cambridge, MA 02138–2902; orcid.org/0000-0003-3352-5383.

Matthew Nava – Department of Chemistry and Chemical Biology, Harvard University, 12 Oxford Street, Cambridge, MA 02138–2902; orcid.org/0000-0001-6575-1153

Notes

The authors declare no competing financial interests

ACKNOWLEDGMENTS

This work was supported by the National Science Foundation under grant CHE-1855531. M.I.G. acknowledges the Arnold and Mabel Beckman Foundation for an Arnold O. Beckman Postdoctoral Fellowship. NSF's ChemMatCARS Sector 15 is supported by the Divisions of Chemistry and Materials Research, National Science Foundation, under grant number CHE-1834750. Use of the Advanced Photon Source, an Office of Science User Facility operated for the U.S. Department of Energy (DOE) Office of Science by Argonne National Laboratory, was supported by the DOE under Contract No. DE-AC02-06CH11357.

REFERENCES

(1) Shaw, M. H.; Twilton, J.; MacMillan, D. W. C. Photoredox Catalysis in Organic Chemistry. *J. Org. Chem.* **2016**, *81*, 6898–6926.

(2) Romero, N. A.; Nicewicz, D. A. Organic Photoredox Catalysis. *Chem. Rev.* **2016**, *116*, 10075–10166.

(3) Huang, H.; Lambert, T. H. Electrophotocatalytic SNAr Reactions of Unactivated Aryl Fluorides at Ambient Temperature and Without Base. *Angew. Chem. Int. Ed.* **2020**, *59*, 658–662.

(4) Huang, H.; Strater, Z. M.; Rauch, M.; Shee, J.; Sisto, T. J.; Nuckolls, C.; Lambert, T. H. Electrophotocatalysis with a Trisaminocyclopropenium Radical Dication. *Angew. Chem. Int. Ed.* **2019**, *58*, 13318–13322.

(5) Shen, T.; Lambert, T. H. Electrophotocatalytic Diamination of Vicinal C–H Bonds. *Science* **2021**, *371*, 620–626.

(6) Huang, H.; Strater, Z. M.; Lambert, T. H. Electrophotocatalytic C–H Functionalization of Ethers with High Regioselectivity. *J. Am. Chem. Soc.* **2020**, *142*, 1698–1703.

(7) Cowper, N. G. W.; Chernowsky, C. P.; Williams, O. P.; Wickens, Z. K. Potent Reductants via Electron-Primed Photoredox Catalysis: Unlocking Aryl Chlorides for Radical Coupling. *J. Am. Chem. Soc.* **2020**, *142*, 2093–2099.

(8) MacKenzie, I. A.; Wang, L.; Onuska, N. P. R.; Williams, O. F.; Begam, K.; Moran, A. M.; Dunietz, B. D.; Nicewicz, D. A. Discovery and Characterization of an Acridine Radical Photoreductant. *Nature* **2020**, *580*, 76–80.

(9) Kim, H.; Kim, H.; Lambert, T. H.; Lin, S. Reductive Electrophotocatalysis: Merging Electricity and Light to Achieve Extreme Reduction Potentials. *J. Am. Chem. Soc.* **2020**, *142*, 2087–2092.

(10) Cole, J. P.; Chen, D.; Kudisch, M.; Pearson, R. M.; Lim, C.-H.; Miyake, G. M. Organocatalyzed Birch Reduction Driven by Visible Light. *J. Am. Chem. Soc.* **2020**, *142*, 13573–13581.

(11) Costentin, C.; Fortage, J.; Collomb, M.-N. Electrophotocatalysis: Cyclic Voltammetry as an Analytical Tool. *J. Phys. Chem. Lett.* **2020**, *11*, 6097–6104.

(12) Fox, M. A. The Photoexcited States of Organic Anions. *Chem. Rev.* **1979**, *79*, 253–273.

(13) Shukla, S. S.; Rusling, J. F. Photoelectrocatalytic Reduction of 4-Chlorobiphenyl Using Anion Radicals and Visible Light. *J. Phys. Chem.* **1985**, *89*, 3353–3358.

(14) Fujitsuka, M.; Kim, S. S.; Lu, C.; Tojo, S.; Majima, T. Intermolecular and Intramolecular Electron Transfer Processes from Excited Naphthalene Diimide Radical Anions. *J. Phys. Chem. B* **2015**, *119*, 7275–7282.

(15) Fujitsuka, M.; Majima, T. Reaction Dynamics of Excited Radical Ions Revealed by Femtosecond Laser Flash Photolysis. *J. Photochem. Photobiol. C Photochem. Rev.* **2018**, *35*, 25–37.

(16) Fujita, M.; Ishida, A.; Majima, T.; Takamuku, S. Lifetimes of Radical Anions of Dicyanoanthracene, Phenazine, and Anthraquinone in the Excited State from the Selective Electron-Transfer Quenching. *J. Phys. Chem.* **1996**, *100*, 5382–5387.

(17) Breslin, D. T.; Fox, M. A. Excited-State Behavior of Thermally Stable Radical Ions. *J. Phys. Chem.* **1994**, *98*, 408–411.

(18) Gosztola, D.; Niemczyk, M. P.; Svec, W.; Lukas, A. S.; Wasielewski, M. R. Excited Doublet States of Electrochemically Generated Aromatic Imide and Diimide Radical Anions. *J. Phys. Chem. A* **2000**, *104*, 6545–6551.

(19) Gumy, J. C.; Vauthey, E. Investigation of the Excited-State Dynamics of Radical Ions in the Condensed Phase Using the Picosecond Transient Grating Technique. *J. Phys. Chem. A* **1997**, *101*, 8575–8580.

(20) Zinchenko, K. S.; Ardana-Lamas, F.; Seidu, I.; Neville, S. P.; Van Der Veen, J.; Lanfaloni, V. U.; Schuurman, M. S.; Wörner, H. J. Sub-7-Femtosecond Conical-Intersection Dynamics Probed at the Carbon K-Edge. *Science* **2021**, *371*, 489–494.

(21) Martinez, J. F.; La Porte, N. T.; Wasielewski, M. R. Electron Transfer from Photoexcited Naphthalene Diimide Radical Anion to Electrocatalytically Active Re(bpy)$(CO)_3$Cl in a Molecular Triad. *J. Phys. Chem. C* **2018**, *122*, 2608–2617.

(22) Christensen, J. A.; Phelan, B. T.; Chaudhuri, S.; Acharya, A.; Batista, V. S.; Wasielewski, M. R. Phenothiazine Radical Cation Excited States as Super-Oxidants for Energy-Demanding Reactions. *J. Am. Chem. Soc.* **2018**, *140*, 5290–5299.

(23) Eriksen, J.; Joergensen, K. A.; Linderberg, J.; Lund, H. Electron-Transfer Fluorescence Quenching of Radical Ions. Experimental Work and Theoretical Calculations. *J. Am. Chem. Soc.* **1984**, *106*, 5083–5087.

(24) Eriksen, J.; Lund, H.; Nyvad, A. I. Electron-Transfer Fluorescence Quenching of Radical Ions. *Acta Chem. Scand.* **1983**, *37b*, 459–466.

(25) Chakraborty, B.; Menezes, P. W.; Driess, M. Beyond CO_2 Reduction: Vistas on Electrochemical Reduction of Heavy Non-Metal Oxides with Very Strong E–O Bonds (E = Si, P, S). *J. Am. Chem. Soc.* **2020**, *142*, 14772–14788.

(26) Meisenheimer, J. Ueber Reactionen Aromatischer Nitrokorper. *Justus Liebig* **1902**, *323*, 205–242.

(27) Jackson, C. J.; Gazzolo, F. H. On Certain Colored Substances Derived from Nitro Compounds. Third Paper. *Proc. Am. Acad. Arts Sci.* **1900**, *35*, 263–281.

(28) Savéant, J-M.; Costentin, C. Elements of Molecular and Biomolecular Electrochemistry. 2nd Ed. Wiley, Hoboken, NJ, 2019.

(29) Tian, X.; Karl, T. A.; Reiter, S.; Yakubov, S.; de Vivie-Riedle, R.; König, B.; Barham, J. P. Electro-Mediated PhotoRedox Catalysis for Selective C(sp^3)–O Cleavages of Phosphinated Alcohols to Carbanions. *Angew. Chem. Int. Ed.* **2021**, doi 10.1002/anie.202105895.

(30) Guha, S.; Saha, S. Fluoride Ion Sensing by an Anion-π Interaction. *J. Am. Chem. Soc.* **2010**, *132*, 17674–17677.

(31) Wentz, H. C.; Skorupskii, G.; Bonfim, A. B.; Mancuso, J. L.; Hendon, C. H.; Oriel, E. H.; Sazama, G. T.; Campbell, M. G. Switchable Electrical Conductivity in a Three-Dimensional Metal-Organic Framework: Via Reversible Ligand n-Doping. *Chem. Sci.* **2020**, *11*, 1342–1346.

(32) Neumann, C. N.; Hooker, J. M.; Ritter, T. Concerted Nucleophilic Aromatic Substitution with $^{19}F^-$ and $^{18}F^-$. *Nature* **2016**, *534*, 369–373.

(33) Lenke, H.; Knackmuss, H. J. Initial Hydrogenation during Catabolism of Picric Acid by Rhodococcus Erythropolis HL 24-2. *Appl. Environ. Microbiol.* **1992**, *58*, 2933–2937.

(34) Saha, S. Anion-Induced Electron Transfer. *Acc. Chem. Res.* **2018**, *51*, 2225–2236.

(35) Bélanger-Chabot, G.; Ali, A.; Gabbaï, F. P. On the Reaction of Naphthalene Diimides with Fluoride Ions: Acid/Base versus Redox Reactions. *Angew. Chem. Int. Ed.* **2017**, *56*, 9958–9961.

(36) Ghosh, I.; Ghosh, T.; Bardagi, J. I.; Konig, B. Reduction of Aryl Halides by Consecutive Visible Light-Induced Electron Transfer Processes. *Science* **2014**, *346*, 725–728.

(37) Marchini, M.; Gualandi, A.; Mengozzi, L.; Franchi, P.; Lucarini, M.; Cozzi, P. G.; Balzani, V.; Ceroni, P. Mechanistic Insights into Two-Photon-Driven Photocatalysis in Organic Synthesis. *Phys. Chem. Chem. Phys.* **2018**, *20*, 8071–8076.

(38) Zeman, C. J.; Kim, S.; Zhang, F.; Schanze, K. S. Direct Observation of the Reduction of Aryl Halides by a Photoexcited Perylene Diimide Radical Anion. *J. Am. Chem. Soc.* **2020**, *142*, 2204–2207.

(39) Janzen, E. G.; Rudy, B. C.; Lopp, I. G.; Happ, J. W. Chemiluminescent Oxygenation of 9,10-Dicyanoanthracene Radical Anion. *Chem. Commun.* **1970**, 491–492.

(40) Schmalzbauer, M.; Marcon, M.; König, B. Excited State Anions in Organic Transformations. *Angew. Chem. Int. Ed.* **2021**, *60*, 6270–6292.

(41) Schmalzbauer, M.; Svejstrup, T. D.; Fricke, F.; Brandt, P.; Johansson, M. J.; Bergonzini, G.; König, B. Redox-Neutral Photocatalytic C–H Carboxylation of Arenes and Styrenes with CO_2. *Chem* **2020**, *6*, 2658–2672.

(42) Schmalzbauer, M.; Ghosh, I.; König, B. Utilising Excited State Organic Anions for Photoredox Catalysis: Activation of (Hetero)Aryl Chlorides by Visible Light-Absorbing 9-Anthrolate Anions. *Faraday Discuss.* **2019**, *215*, 364–378.

Table of Contents